Hindawi Publishing Corporation
International Journal of Antennas and Propagation
Volume 2014, Article ID 501025, 8 pages
http://dx.doi.org/10.1155/2014/501025

Research Article

Low-Complexity Spatial-Temporal Filtering Method via Compressive Sensing for Interference Mitigation in a GNSS Receiver

Chung-Liang Chang[1] and Guo-Shing Huang[2]

[1] *Department of Biomechatronics Engineering, National Pingtung University of Science and Technology, No. 1, Shuefu Road, Neipu, Pingtung County 91201, Taiwan*
[2] *Department of Electronic Engineering, National Chin-Yi University of Technology, No. 57, Sec. 2, Zhongshan Road, Taiping District, Taichung 41170, Taiwan*

Correspondence should be addressed to Chung-Liang Chang; chungliang@mail.npust.edu.tw

Received 17 February 2014; Revised 17 April 2014; Accepted 22 April 2014; Published 28 May 2014

Academic Editor: Hon Tat Hui

A compressive sensing based array processing method is proposed to lower the complexity, and computation load of array system and to maintain the robust antijam performance in global navigation satellite system (GNSS) receiver. Firstly, the spatial and temporal compressed matrices are multiplied with array signal, which results in a small size array system. Secondly, the 2-dimensional (2D) minimum variance distortionless response (MVDR) beamformer is employed in proposed system to mitigate the narrowband and wideband interference simultaneously. The iterative process is performed to find optimal spatial and temporal gain vector by MVDR approach, which enhances the steering gain of direction of arrival (DOA) of interest. Meanwhile, the null gain is set at DOA of interference. Finally, the simulated navigation signal is generated offline by the graphic user interface tool and employed in the proposed algorithm. The theoretical analysis results using the proposed algorithm are verified based on simulated results.

1. Introduction

The global navigation satellite system (GNSS) has been widely used in military, satellite attitude control mission, and civilian applications such as vehicle positioning and mobile navigation. The user can utilize a GNSS receiver to know the current location, including longitude, latitude, and time. At present, two bands, L1 and L2, are employed in global positioning system (GPS) to meet the high-precision positioning demands such as during military operations. However, most of low cost GNSS receivers are equipped with only single frequency (L1) band, which results in low antijam capability. The accuracy and precision of user location can be affected by unintentional or intentional interferences. Thus, the antijam module needs to be embedded in the receiver to maintain positioning performance. The antenna array and pre- or postprocessing techniques are common methods to mitigate or cancel interferences. Among them, only antenna array technique can obtain the best antijam performance (about 30 to 50 dB). However, the pre- or postprocessing techniques are widely used in current interior GNSS receiver design because of low cost and complexity. The spatial-temporal adaptive processing (STAP) techniques have been proposed to perform 2D filtering on radar or navigation signals to mitigate narrowband/wideband (NB/WB) interferences, multipath, and other uncertainties [1–7]. Nevertheless, it is necessary to increase the number of antennas and time delay elements to obtain better antijam performance for antenna array processing [8]. Thus, the major challenges for a perfect GNSS receiver design include reducing the weight, complexity, and computation time in antenna array processing to maintain good acquisition performance and interference resistance.

In 2008, Candes and Wakin proposed a compressive sensing approach for acquiring the sparse signal and reconstruction from the compressed measurements [9].

This technique includes three components: the sparse transform of the signal, including ordered discrete Hadamard transform (DHT) and discrete cosine transform (DCT), the sparse signal with linear/nonlinear measurement, and signal reconstruction, such as robust uncertainty principles [10], orthogonal matching pursuit method [11], and iterative thresholding [12]. This technique has been widely used in biomedicine, radar, wireless communication, and other field applications [13–15]. The compressive sensing (CS) based approach has been applied to array processing to estimate Doppler-direction-of-arrival (DDOA) for beamforming by using less number of array antennas and less number of samples/snapshots for each antenna [16, 17]. In this paper, the CS based spatial-temporal array processing with minimum variance distortionless response (MVDR) is proposed to mitigate the narrowband/wideband interferences. The time delay elements, different from the previous research [18], are added into each antenna, allowing us to effectively mitigate interference through STAP compressed measurement using a MVDR beamformer.

2. Methodology

2.1. Signal Model. Assume that lth navigation satellite signal z_l is received from the antenna frontend at kth ($k = 1, 2, \ldots, K$) time instant, which can be represented as follows:

$$r(k) = \sum_{l=1}^{L} \underbrace{\sqrt{\rho_l} D_l(k) C_l(k-\tau_l) \exp\left(j2\pi\left(f_l/F_s\right)k + \varphi_l\right)}_{z_l} + v(k), \tag{1}$$

where L depicts the number of light of sight (LOS) navigation satellite signal in the sky, ρ_l is signal power, D_l and C_l depict the navigation message bit and pseudo random noise (PRN) code of lth satellite with time delay τ_l, f_l represents analog intermediate frequency (IF), and $v(k)$ is interference term which consists of WB/NB interferences and Gaussian noise. $F_s = K/T$ denotes the Nyquist sampling rate (Hz) which is equal to K/T, where T and K denote a short observation and the data length of signal reception, respectively.

As for array processing, the aggregate signal x_n received at nth input of array system of N antenna elements is given by

$$\begin{aligned}\mathbf{x}(k) &= \begin{bmatrix} x_1 & x_2 & \cdots & x_n & \cdots & x_N \end{bmatrix}^H \\ &= \sum_{l=1}^{L} \mathbf{a}_l(\theta_l, \phi_l) z_l(k) + \mathbf{v}'(k),\end{aligned} \tag{2}$$

where x_n denotes the incoming signals on nth antenna element and $\mathbf{v}'$ is an additional interference term of N-dimension. $\mathbf{a}_l$ denotes the array response vector with respect to nth navigation signal source at elevation θ_l and azimuth ϕ_l. Assume that the basic matrix $\mathbf{\Psi}_{\theta,\phi}$ is determined in the angle domain of size $N \times M_\alpha^2$ ($M_\alpha^2 \gg N$) as

$$\mathbf{\Psi}_{\theta,\phi} = \begin{bmatrix} \mathbf{a}_{11}(\theta_1, \phi_1) & \mathbf{a}_{12}(\theta_1, \phi_2) & \cdots & \mathbf{a}_{1M_\alpha}\left(\theta_1, \phi_{M_\alpha}\right) & \mathbf{a}_{21}(\theta_2, \phi_1) & \mathbf{a}_{22}(\theta_2, \phi_2) & \cdots & \mathbf{a}_{M_\alpha M_\alpha}\left(\theta_{M_\alpha}, \phi_{M_\alpha}\right) \end{bmatrix}, \tag{3}$$

where

$$\mathbf{a}_{uv}(\theta_u, \phi_v) = \frac{\begin{bmatrix} 1 & a_1(\theta_u, \phi_v) & a_2(\theta_u, \phi_v) & \cdots & a_{N-1}(\theta_u, \phi_v) \end{bmatrix}^T}{\sqrt{N}}, \tag{4}$$

and M_α represents the number of azimuth and elevation search grid and $\mathbf{a}_{uv}(\theta_u, \phi_v)$ illustrates the steering vector from the direction of arrival at azimuth ϕ_v and elevation θ_u. Meanwhile, the basic matrix $\mathbf{\Psi}_f$ in the frequency domain of size $K \times M_\beta$ ($M_\beta \gg K$) is defined as

$$\begin{aligned}\mathbf{\Psi}_f &= \begin{bmatrix} 1 & \mathbf{f}_1 & \mathbf{f}_2 & \cdots & \mathbf{f}_{M_\beta} \end{bmatrix}, \\ \mathbf{f}_m &= \frac{\begin{bmatrix} 1 & e^{j2\pi(f_m/F_s)} & e^{j4\pi(f_m/F_s)} & \cdots & e^{j2\pi(f_m/F_s)(K-1)} \end{bmatrix}^T}{\sqrt{K}},\end{aligned} \tag{5}$$

where M_β is frequency search grid and $\mathbf{f}_m$ denotes the Fourier basis vector for f_m. Combining (3) and (4), (1) can be rewritten as matrix $\mathbf{X}$ with a size of $N \times K$ and $\overline{x}(n,k)$ as its coefficient on the nth row and the kth column:

$$\mathbf{X} = \mathbf{\Psi}_{\theta,\phi} \mathbf{U} \mathbf{\Psi}_f^T, \tag{6}$$

where $\mathbf{U}$ is a $M_\alpha^2 \times M_\beta$ sparse matrix including J nonzeros coefficients. Assume that the DOA of lth signal at (θ_l, ϕ_l) and Doppler frequency f_l are aligned on the search grids (if M_α and M_β are large enough), indexed by p_l and m_l, respectively, and $\mathbf{U}(p_l, m_l) = \sqrt{\rho_l} D_l C_l$.

2.2. Compressive Spatial-Temporal Array Processing. Figure 1 depicts the proposed CS based array system architecture. Firstly, the spatial compressed matrix $\mathbf{\Phi}_p$ with a size of $P \times N$ ($P < N$) is determined to reduce the original dimension N of spatial array matrix to a lower dimension P of array matrix. Then, P channel analog data is converted to digital samples instead of original N channel data. Subsequently, the analog to digital converter (ADC) with a Nyquist sampling rate is changed into an analog to information (A2I) converter with a sub-Nyquist sampling rate by a switch. The original signal

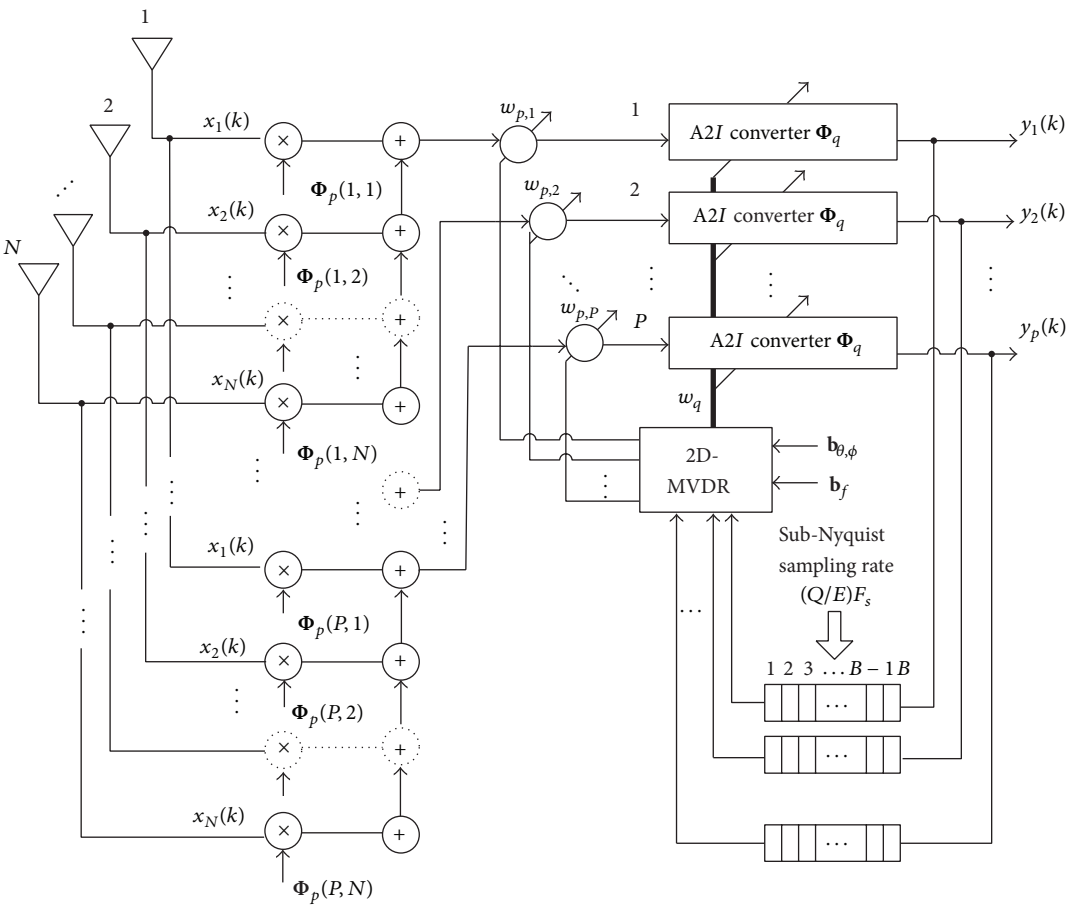

Figure 1: Block diagram of CS based spatial-temporal array system.

samples K of temporal domain are divided into $B = K/E$ block due to A2I converter to carry out the block-wise compression. The temporal compression matrix $\mathbf{\Phi}_q$ of size $Q \times E$ ($Q < E$) is defined and indicated as a sampling process in A2I converter with Q/E ratio of Nyquist sampling rate. The A2I converter performs subsampling process that transforms the E samples per block to Q samples; it results in total $K' = BQ$ samples for output. The independent and identically distributed (i.i.d.) coefficients in spatial-temporal compression matrices ($\mathbf{\Phi}_p$ and $\mathbf{\Phi}_q$) are assumed to be randomly distributed (e.g., Bernoulli, Gaussian, etc.), which satisfies restricted isometry property (RIP) with high probability [19]. During the hardware implementation process, the on/off selection switch or a phase shifter/attenuator can be used to implement the multiplication with coefficients from spatial compressive matrix $\mathbf{\Phi}_p$. The mixer and integrators can be used to be implemented in multiplication with coefficients from $\mathbf{\Phi}_q$ due to the fact that A2I converter operates on the analog signal after ADC. The A2I converter then outputs the digital signal. The smaller P and Q are, the lower the implementation complexity of A2I converter is. To simplify the notation, the digital baseband version is employed in all equations. Assume that the array signal at kth index in (6) is rewritten as

$$\mathbf{X} = \left[\mathbf{X}_1 \;\; \mathbf{X}_2 \;\; \cdots \;\; \mathbf{X}_i \;\; \cdots \;\; \mathbf{X}_B\right]_{N \times K}, \tag{7}$$

where $i = 1, 2, \ldots, b, \ldots, B$ denotes the block index, and the length of each block is E, which is equal to $1/B$ coarse acquisition (C/A) code period. $\mathbf{X}_i$ is the uncompressed signal of size $N \times E$:

$$\mathbf{X}_i = \left[\mathbf{x}\left(((b-1)E+1)T_s\right) \;\; \mathbf{x}\left(((b-1)E+2)T_s\right) \;\; \cdots \;\; \mathbf{x}\left(((b-1)E+E)T_s\right)\right]_{N \times E}. \tag{8}$$

After the compressed spatial-temporal process, (7) and (8) become

$$\mathbf{Z} = \left[\mathbf{Z}_1 \;\; \mathbf{Z}_2 \;\; \cdots \;\; \mathbf{Z}_B\right]_{P\times K'} \tag{9}$$

$$\mathbf{Z}_i = \left[\mathbf{\Phi}_p \mathbf{X}_i \mathbf{\Phi}_q^H\right]_{P\times Q}, \tag{10}$$

where $\mathbf{Z}_i$ indicate the ith compressive spatial-temporal matrix with a size of $P \times Q$. Then (9) can be rewritten as

$$\mathbf{Z} = \mathbf{\Phi}_a \mathbf{X}\left(\mathbf{I_B} \otimes \mathbf{\Phi}_b\right)^T = \overline{\mathbf{\Psi}}_{\theta,\phi} \mathbf{U} \overline{\mathbf{\Psi}}_f^T, \tag{11}$$

where $\overline{\mathbf{\Psi}}_{\theta,\phi}$ and $\overline{\mathbf{\Psi}}_f$ denote compressed angle and frequency basis matrix, respectively.

Consider

$$\begin{aligned} \overline{\mathbf{\Psi}}_{\theta,\phi} &= \mathbf{\Phi}_a \mathbf{\Psi}_{\theta,\phi}, \\ \overline{\mathbf{\Psi}}_f &= \left(\mathbf{I_B} \otimes \mathbf{\Phi}_b\right) \mathbf{\Psi}_f. \end{aligned} \tag{12}$$

Assume frequency basis matrix $\overline{\mathbf{\Psi}}_f$ is divided into B submatrices, each with Q rows. Then, the matrix $\overline{\mathbf{\Psi}}_{f,i}$ depicts ith submatrix of $\overline{\mathbf{\Psi}}_f$. Equation (10) can be rewritten as

$$\mathbf{Z}_i = \overline{\mathbf{\Psi}}_{\theta,\phi} \mathbf{U} \overline{\mathbf{\Psi}}_{f,i}^T. \tag{13}$$

2.3. 2-Dimensional MVDR Beamformer. Assume that the DOA of a desired signal and Doppler frequency are known a priori. The optimum MVDR beamformers $\mathbf{w}_p$ and $\mathbf{w}_q$ can be found by employing iterative procedures. Thus, spatial gain vector $\mathbf{w}_p$ can be found by solving the constrained minimization problem:

$$\begin{aligned} \arg\min_{\mathbf{w}_p} \quad & \mathbf{w}_p^H \mathbf{R} \mathbf{w}_p \\ \text{subject to} \quad & \mathbf{w}_p^H \mathbf{b}_{\theta,\phi} = 1, \end{aligned} \tag{14}$$

where $\mathbf{b}_{\theta,\phi,P\times 1} = \left[1 \;\; a_1 \;\; \cdots \;\; a_b \;\; \cdots \;\; a_{P-1}\right]^T$ depicts the null steering vector with the coefficient a_b, $\mathbf{R}_{P\times P} = \overline{\mathbf{Z}}\,\overline{\mathbf{Z}}^H/B$, and $\overline{\mathbf{Z}}_{P\times B} = \mathbf{Z}_{P\times BQ}(\mathbf{I}_B \otimes \mathbf{w}^*_{q,Q\times 1})$ with a size of $P \times B$. The Lagrange multiplier method [20] is utilized to solve minimization problem in (14) and the solution of MVDR beamformer is as follows:

$$\mathbf{w}_p = \frac{\mathbf{R}^{-1}\mathbf{b}_{\theta,\phi}}{\mathbf{b}_{\theta,\phi}^H \mathbf{R}^{-1} \mathbf{b}_{\theta,\phi}}. \tag{15}$$

In addition, the temporal gain vector $\mathbf{w}_q$ can also be found via constraint minimization problem:

$$\begin{aligned} \arg\min_{\mathbf{w}_q} \quad & \mathbf{w}_q^H \mathbf{R}' \mathbf{w}_q \\ \text{subject to} \quad & \mathbf{w}_q^H \mathbf{b}_f\left(\omega_0\right) = 1, \\ \mathbf{b}_{f,Q\times 1}\left(\omega_0\right) &= \left[1 \;\; e^{-j\omega_0} \;\; \cdots \;\; e^{-j(Q-1)\omega_0}\right]^T, \end{aligned} \tag{16}$$

where ω_0 is angular frequency of special interest, $[\cdot]^T$ denotes transposition without conjugation, and $\mathbf{R}'_{Q\times Q} = \overline{\mathbf{Z}}'\,\overline{\mathbf{Z}}'^H/B$, $\mathbf{Z}' = \left[\mathbf{Z}_1^H \;\; \mathbf{Z}_2^H \;\; \cdots \;\; \mathbf{Z}_B^H\right]_{Q\times BP}$, and $\overline{\mathbf{Z}}'_{Q\times B} = \mathbf{Z}'_{Q\times BP}(\mathbf{I}_B \otimes \mathbf{w}^*_{p,P\times 1})$ with a size of $Q \times B$. Meanwhile, the method of Lagrange multiplier is employed to solve minimization problem in (16) and the solution is explicitly given by the MVDR beamformer:

$$\mathbf{w}_q = \frac{\mathbf{R}'^{-1}\mathbf{b}_f}{\mathbf{b}_f^H \mathbf{R}'^{-1} \mathbf{b}_f}. \tag{17}$$

The gain vector $\mathbf{w}_p$ is a beamformer for (θ_l, ϕ_l) and $\mathbf{w}_q$ is a certain DDOA for beamforming.

The spatial correlation matrix $\mathbf{R}$ is calculated to obtain the new gain vector $\mathbf{w}_p$. Therefore, the $\mathbf{w}_q$ is utilized as a bandpass filter centered at frequency f_m to acquire the filtered signal $\overline{\mathbf{Z}}$. The temporal correlation matrix $\mathbf{R}'$ is calculated to find the new gain vector $\mathbf{w}_q$. Consequently, to compute the temporal gain vector, $\mathbf{w}_p$ is used as spatial filter steered to (θ_l, ϕ_l) to obtain the beamformed signal $\overline{\mathbf{Z}}'$. The MVDR method is utilized to solve $\mathbf{w}_p$ and $\mathbf{w}_q$ which looks for a spatial-temporal filter to reject the great amount of out-of-band power while passing component at angle (θ_l, ϕ_l) or frequency f_m with no distortion. In the following, assume that the compressed spatial-temporal gain vector $\mathbf{w}_{PQ\times 1}$ is equal to $\mathbf{w}_q \otimes \mathbf{w}_p$, the total output power of the system is $\mathbf{w}^H \mathbf{\Lambda} \mathbf{w}$, where $\mathbf{\Lambda}_{PQ\times PQ} = \mathbf{R} \otimes \mathbf{R}'$, and the corresponding optimal signal to interference-plus-noise ratio (SINR) is given by

$$\mathrm{SINR}_{\mathrm{opt}} = \sigma_d^2 \mathbf{b}^H \mathbf{\Lambda}^{-1} \mathbf{b}, \tag{18}$$

where $\mathbf{b}_{PQ\times 1} = \mathbf{b}_f \otimes \mathbf{b}_{\theta,\phi}$ denotes PQ-dimensional compressed spatial-temporal steering vector of the special interest and σ_d^2 is signal power of interest. The minimum sum of error square is as follows:

$$\xi_{\min}^2 = 1 - \mathbf{w}^H \mathbf{\Lambda} \mathbf{w}. \tag{19}$$

2.4. Performance Comparison. This section explores the difference between proposed method and other traditional STAP algorithms in terms of system complexity and computation efficiency. The advantage of proposed compression method is that it can reduce the computation time during matrix multiplication of STAP algorithms and also the logic gate count. The performance difference of reduced-rank power minimization (PM) [21], MSNWF [22], MVDR [23], and compressive MVDR (C-MVDR) of beamforming algorithm with regard to convergence rate, steady state error, numerical stability, and system complexity is demonstrated and compared in Table 1. It can also be concluded that array signal after the compression process passing through MVDR beamformer can yield better beam pattern. The error convergence rate of proposed method is superior to that without compression. Also, C-MVDR and MSNWF both are lower in steady state error in contrast to MVDR and reduced-rank PM without compression. The system complexity of proposed method is lower than that of other methods. Table 2

Table 1: Performance comparison of different beamforming algorithms.

Performance criteria	Algorithm			
	Reduced-rank PM	MSNWF	MVDR	C-MVDR
Converge rate	Fast	Fast	Medium	Fast
Steady state error	Large	Small	Medium	Small
Numerical stability	Unstable (CS, PC principle)	Stable	Stable	Stable (satisfy RIP condition)
System complexity	Medium	Medium (depend on J)	High	Low (depend on P and Q)

Table 2: Complexity comparison of STAP algorithms in different update procedures.

Algorithm	Evaluation factors	Intermediate Con-strained matrix	Update weight vector	Total complexity	Computation load (per snapshot)
Reduced-rank PM	MUX	$NEJ + J^2 + J$	$NEJ^2 + NEJ + J$	$NEJ^2 + 2NEJ + J^2 + 2J$	$O[NEJ]$
	ADD	$3NEJ - 2NE + J^2 - 1$	$3NEJ - NE - J - 1$	$6NEJ - 3NE + J^2 - J - 2$	
	MEM	$2NE$	$2NE + NEJ + J$	$NEJ + 4NE + J$	
MSNWF	MUX	$NEJ + J$	$NEJ + 2J$	$2NEJ + 3J$	$O[NEJ]$
	ADD	NEJ	$NEJ + 2J$	$2NEJ + 2J$	
	MEM	NE	$NE + 2$	$2NE + 2$	
MVDR	MUX	$3NE$	$3(NE)^3 + (NE)^2$	$3(NE)^3 + (NE)^2 + 3NE$	$O\left[(NE)^3\right]$
	ADD	$2(NE)^2 - 2NE$	$3(NE)^3 - 2(NE)^2 - NE$	$3(NE)^3 - 3NE$	
	MEM	$(NE)^2 + E^2$	NE	$(NE)^2 + E^2 + NE$	
C-MVDR	MUX	$3PQ$	$3(PQ)^3 + (PQ)^2$	$3(PQ)^3 + (PQ)^2 + 3PQ$	$O\left[(PQ)^3\right]$
	ADD	$2(PQ)^2 - 2PQ$	$3(PQ)^3 - 2(PQ)^2 - PQ$	$3(PQ)^3 - 3PQ$	
	MEM	$(PQ)^2 + Q^2$	PQ	$(PQ)^2 + Q^2 + PQ$	

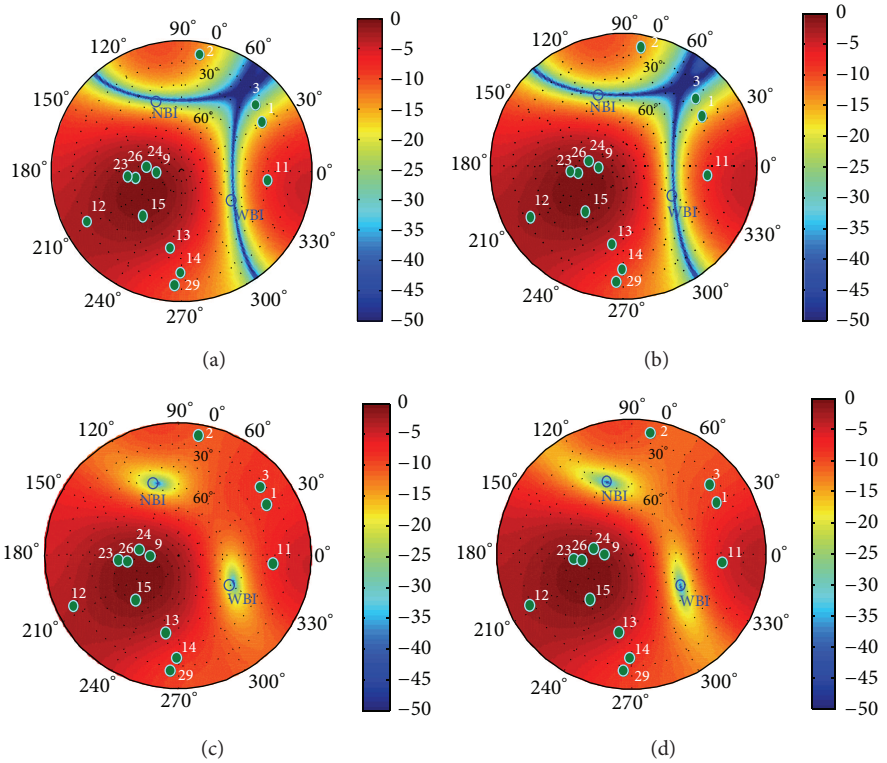

Figure 2: The gain patterns with and without compression measurement ($K' = 3600$, $Q = 17$, and $B = 200$); (a) without compression measurement (4 antennas); (b) with compression measurement (4 antennas); (c) without compression measurement (9 antennas); (d) with compression measurement (9 antennas).

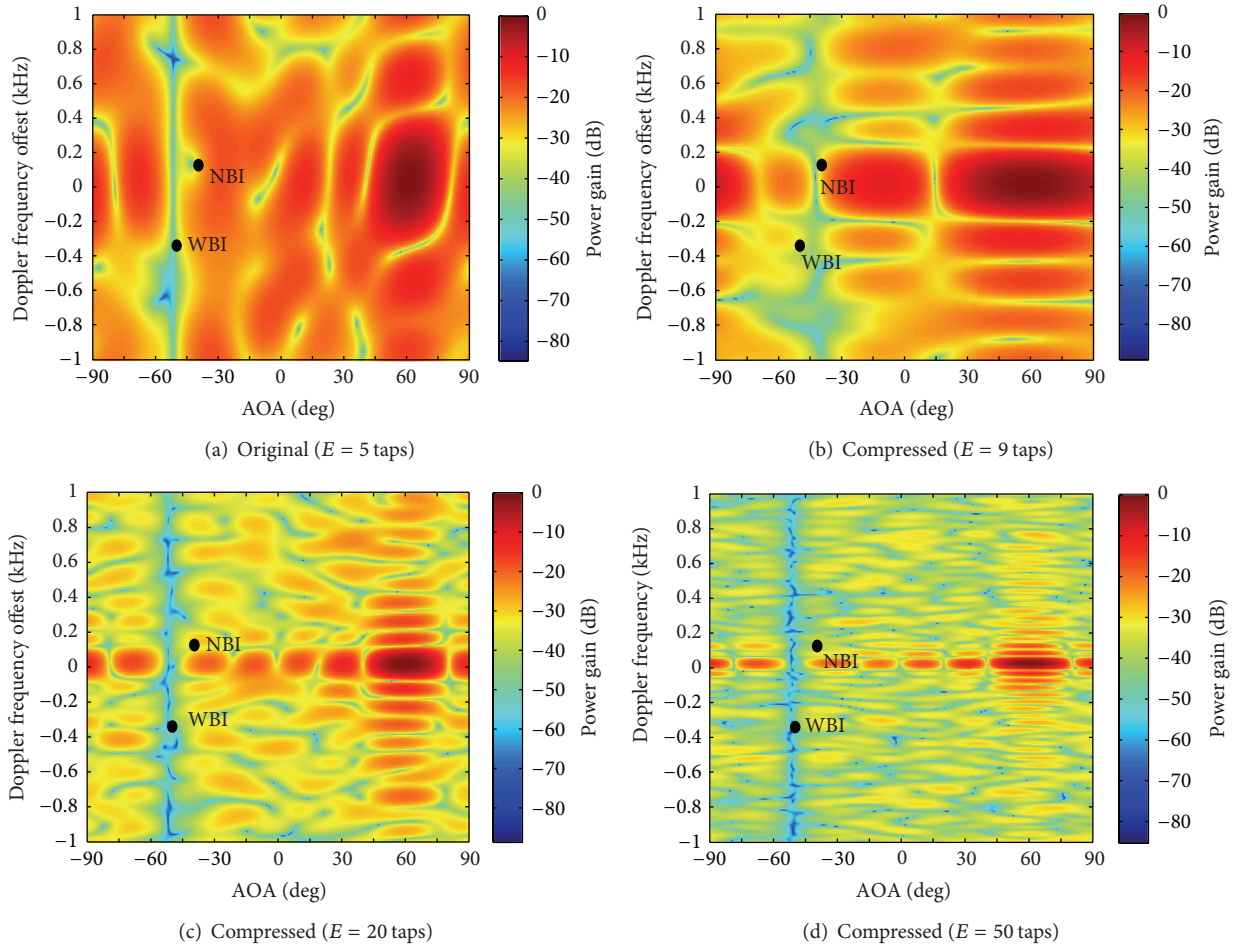

FIGURE 3: The angle-frequency spectrum with and without compression measurement ($K'/K = 0.7$); (a) without compression measurement; (b) with compression measurement under 9 delay taps; (c) with compression measurement under 20 delay taps; (d) with compression measurement under 50 delay taps.

illustrates the relation between system complexities of different STAP algorithms in different update procedures [24]. The implementation difference of each algorithm is assessed using the number of multiplier (MUX), adder (ADD), and data memory (MEM). Table 2 shows that, with the reduction of N and E, the total computation time of C-MVDR will decrease by cube root as opposed to that of MVDR. In addition, the total hardware implementation complexity will reduce a lot.

3. Simulation Results

The analysis and assessment of the proposed system are illustrated and verified in this section. Uniform rectangular array (URA) with half of wavelength spacing is utilized in the proposed system under no mutual coupling condition. The number of antenna elements is associated with the number of narrowband/wideband interferences that can be cancelled by the STAP algorithm. All antennas are assumed to be ideal and have an omnidirectional radiation pattern. In general, the number of broadband interferences that can be eliminated by the spatial-temporal filtering corresponds to $P-1$ [4]. Assume that IF frequency of GNSS signal is 1.25 MHz with a sampling rate of $F_s = 5$ MHz and the reception data length is $T = 1$ ms (equal to $K = F_sT = 5000$ samples). The compression matrices $\mathbf{\Phi}_p$ and $\mathbf{\Phi}_q$ are generated using random Gaussian distribution. The Monte Carlo simulation is conducted for 500 runs to assess the performance of proposed system under jammed environment.

First, the GPS YUMA almanacs data [25] and MATLAB software are employed to simulate the distribution of LOS satellites (total thirteen) in the sky. All GPS satellite signals are received at different azimuth and elevation with −15~ −10 dB SNR in average. Assume that incident direction of wideband interference is at azimuth 330 degree and 53 elevation degree and the direction of arrival of narrowband interference is at azimuth 110 degree and 38 elevation degree. All the INR of interference is set at 30 dB. The number of tap delay element is $B = 10$. Figures 2(a) and 2(b) show the 3D gain pattern as a function of azimuth and elevation angle with and without compression measurement under 4 antennas, respectively. The spatial and temporal compression ratio is set as $\kappa = 0.75$ and $\eta = 0.72$ ($K' = 3600$, $Q = 17$, and $B = 200$), respectively. Figures 2(a) and 2(b) illustrate that both methods can effectively mitigate interference. In particular,

Figure 2(b) shows that the proposed method yields better wideband and narrowband interference mitigation performance. When the antenna number is increased to 9 and the spatial and temporal compression ratio is set as $\kappa = 0.75$ and $\eta = 0.72$ ($K' = 3600$, $Q = 17$, and $B = 200$), respectively, a null has been steered toward its DOA in a particular frequency (−47.3 dB for WBI and −45.1 dB for NBI) for each interference (see Figures 2(c) and 2(d)). Thus, the GNSS signals arriving from the same direction can still be distinguished in the frequency domain by a compression spatial-temporal process. For the wideband interference, a null should be placed in its entire frequency band (see Figure 3).

In Figure 3, at an elevation of 53 degree where the wideband interference is received, a null is steered toward that direction for all frequencies. Meanwhile, increasing the number of delay tap can obtain the deep null gain toward interference direction. However, the increasing number of time delay taps will result in more sidelobes within the Doppler frequency range (±0.2 KHz) of the desired signal. When the estimation of AOA and Doppler shift is inaccurate, the directivity outputs SINR, which can be observed in Figure 4. However, the increasing number of time delay taps will result in more sidelobes within the Doppler frequency range (±0.2 KHz) of the desired signal. When the estimation of AOA and Doppler shift is inaccurate, the directivity gain of the desired signal will reduce a lot, which will also reduce output SINR, as observed in Figure 4.

A comparison of the two realizations in terms of SINR improvement varying with the number of delay tap is depicted in Figure 4. The SINR improvement is defined as the difference between the output and input SINR [4, 26]. It is found that increasing the number of delay taps continuously does not improve the antijam performance, which simultaneously denotes output SINR. It is due to the increment of time delay taps that can lead to the desired signal component to be partially mitigated or cancelled, which results in poor SINR improvement performance. Selecting the appropriate number of delay taps is important to enhance system antijam performance.

The comparison of hardware implementation complexity of proposed system and traditional STAP under different space compression ratio and time compression ratio is illustrated in Figure 5. The definition of total complexity is the sum of the number of adders, subtractors, and multipliers. This value indicates that the hardware implementation cost will be lower if the space and time compression ratio is lower. Nevertheless, when the space and time compression ratio is below the lower limit, the proposed method fails to mitigate interference. The analysis is feasible if the number of antennas and time delay taps is more than four and five, respectively.

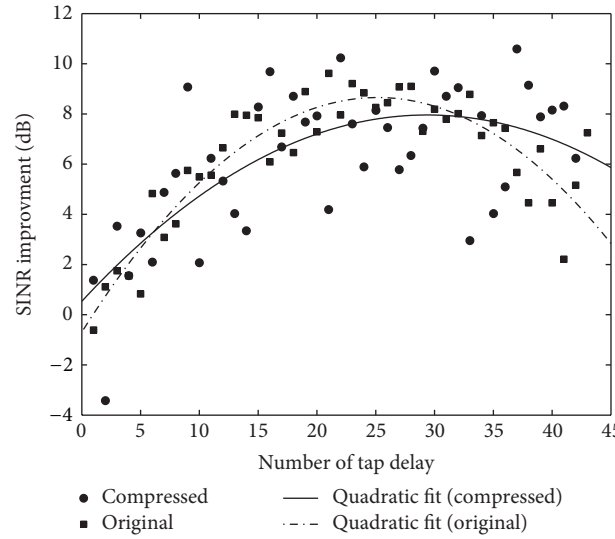

Figure 4: SINR improvement as a function of number of delay taps.

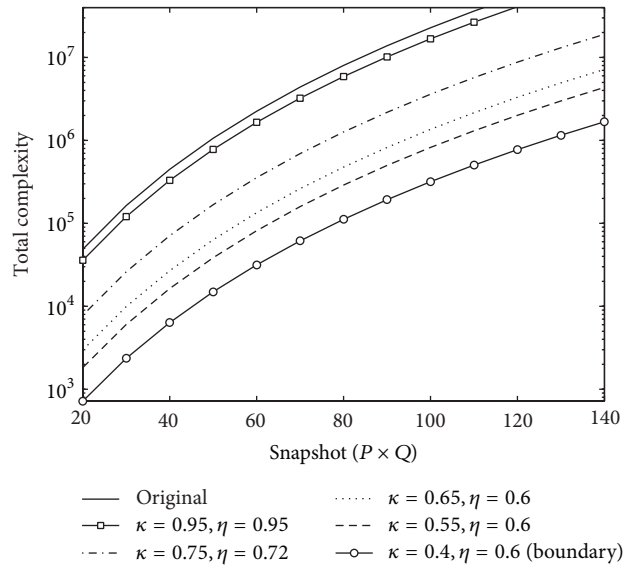

Figure 5: Comparison of hardware complexity under different spatial compression ratio (κ) and temporal compression ratio (η).

4. Conclusions

The combination of compressive spatial-temporal filter with an MVDR processing can mitigate narrowband and wideband interferences in GNSS receiver. As long as spatial-temporal compression matrices can satisfy RIP with high probability and adopt suitable tap number, the proposed method can obtain robust interference mitigation performance. The compression process consumes system computation time that can significantly reduce time after MVDR for a compressed sample. In terms of total system computation time, the use of compression sensors is still better than not using them. The reduced hardware implementation complexity and computation load are more apparent with the increasing number of antennas and time delay taps. In the proposed method, the interferences can be distinguished by a spatial-temporal process within the same DOA of signals and a null gain is placed in its entire frequency band. In addition, the compression method applied to spatial-temporal signal reception model can reduce the hardware complexity and

computation time up to 7.35-fold with a temporal compressive ratio of 0.72 during interference mitigation process under four antenna elements. This method is conducive for future antijam module miniaturization.

Conflict of Interests

The authors declare that there is no conflict of interests regarding the publication of this paper.

Acknowledgment

The authors would like to thank the Ministry of Science and Technology of Taiwan for financial support to this work (Grant no. NSC 102-2221-E-020-007).

References

[1] R. L. Fante and J. J. Vaccaro, "Wideband cancellation of interference in a GPS receive array," *IEEE Transactions on Aerospace and Electronic Systems*, vol. 36, no. 2, pp. 549–564, 2000.

[2] T. K. Sarkar and R. Adve, "Space-time adaptive processing using circular arrays," *IEEE Antennas and Propagation Magazine*, vol. 43, no. 1, pp. 138–143, 2001.

[3] P. Xiong, M. J. Medley, and S. N. Batalama, "Spatial and Temporal Processing for Global Navigation Satellite Systems: the GPS receiver paradigm," *IEEE Transactions on Aerospace and Electronic Systems*, vol. 39, no. 4, pp. 1471–1484, 2003.

[4] C.-L. Chang, "Self-tuning synthesis filter against mutual coupling and interferences for GNSS and its implementation on embedded board," *EURASIP Journal on Advances in Signal Processing*, vol. 2010, Article ID 123625, 2010.

[5] S. Daneshmand, A. Broumandan, J. Nielsen, and G. Lachapelle, "Interference and multipath mitigation utilising a two-stage beamformer for global navigation satellite systems applications," *IET Radar, Sonar & Navigation*, vol. 7, no. 1, pp. 55–66, 2013.

[6] J. F. Degurse, L. Savy, S. Marcos, and J. P. Molinié, "Deterministic aided STAP for target detection in heterogeneous situations," *International Journal of Antennas and Propagation*, vol. 2013, Article ID 826935, 10 pages, 2013.

[7] H. Keshvadi, A. Broumandan, and G. Lachapelle, "Spatial characterization of GNSS multipath channels," *International Journal of Antennas and Propagation*, vol. 2012, Article ID 236464, 15 pages, 2012.

[8] C.-L. Chang, "Multiplexing scheme for anti-jamming global navigation satellite system receivers," *IET Radar, Sonar and Navigation*, vol. 6, no. 6, pp. 443–457, 2012.

[9] E. J. Candes and M. B. Wakin, "An introduction to compressive sampling: a sensing/sampling paradigm that goes against the common knowledge in data acquisition," *IEEE Signal Processing Magazine*, vol. 25, no. 2, pp. 21–30, 2008.

[10] E. J. Candes and T. Tao, "Near-optimal signal recovery from random projections: universal encoding strategies?" *IEEE Transactions on Information Theory*, vol. 52, no. 12, pp. 5406–5425, 2006.

[11] J. A. Tropp and A. C. Gilbert, "Signal recovery from random measurements via orthogonal matching pursuit," *IEEE Transactions on Information Theory*, vol. 53, no. 12, pp. 4655–4666, 2007.

[12] T. Blumensath and M. E. Davies, "Iterative thresholding for saparse approximations," *Journal of Fourier Analysis and Applications*, vol. 14, no. 5-6, pp. 629–654, 2008.

[13] A. Majumdar, R. K. Ward, and T. Aboulnasr, "Compressed sensing based real-time dynamic MRI reconstruction," *IEEE Transactions on Medical Imaging*, vol. 31, no. 12, pp. 2253–2266, 2012.

[14] J. Yang, J. Thompson, X. Huang, T. Jin, and Z. Zhou, "Random-frequency SAR imaging based on compressed sensing," *IEEE Transactions on Geoscience and Remote Sensing*, vol. 51, no. 2, pp. 983–994, 2013.

[15] W. U. Bajwa, J. Haupt, A. M. Sayeed, and R. Nowak, "Compressed channel sensing: a new approach to estimating sparse multipath channels," *Proceedings of the IEEE*, vol. 98, no. 6, pp. 1058–1076, 2010.

[16] A. C. Gürbüz, J. H. McClellan, and V. Cevher, "A compressive beamforming method," in *Proceedings of the IEEE International Conference on Acoustics, Speech and Signal Processing (ICASSP '08)*, pp. 2617–2620, April 2008.

[17] Y. Wang, G. Leus, and A. Pandharipande, "Direction estimation using compressive sampling array processing," in *Proceedings of the IEEE/SP 15th Workshop on Statistical Signal Processing (SSP '09)*, pp. 626–629, Cardiff, UK, September 2009.

[18] C.-L. Chang and G.-S. Huang, "Spatial compressive array processing scheme against multiple narrowband interferences for GNSS," in *Proceedings of the IEEE 1st AESS European Conference on Satellite Telecommunications (ESTEL '12)*, Rome, Italy, October 2012.

[19] R. Baraniuk, M. Davenport, R. DeVore, and M. Wakin, "A simple proof of the restricted isometry property for random matrices," *Constructive Approximation*, vol. 28, no. 3, pp. 253–263, 2008.

[20] S. Hyakin, *Adaptive Filter Theory*, Prentice Hall, Upper Saddle River, NJ, USA, 4th edition, 2002.

[21] Y. T. J. Morton, L. L. Liou, D. M. Lin, J. B. Y. Tsui, and Q. Zhou, "Interference cancellation using power minimization and self-coherence properties of GPS signals," in *Proceedings of the 17th International Technical Meeting of the Satellite Division of the Institute of Navigation (ION GNSS '04)*, pp. 132–143, Long Beach, Calif, USA, September 2004.

[22] W. L. Myrick, M. D. Zoltowski, and J. S. Goldstein, "Anti-jam space-time preprocessor for GPS based on multistage nested Wiener filter," in *Proceedings of the IEEE Military Communications Conference (MILCOM '99)*, pp. 675–681, November 1999.

[23] J. Li, P. Stoica, and Z. Wang, "On robust capon beamforming and diagonal loading," *IEEE Transactions on Signal Processing*, vol. 51, no. 7, pp. 1702–1715, 2003.

[24] C. L. Chang and B. H. Wu, "Analysis of performance and implementation complexity of array processing in anti-jamming GNSS receivers," *Electrical and Electronic Engineering*, vol. 1, no. 2, pp. 79–84, 2011.

[25] T. S. Kelso, "GPS YUMA Almanacs," 2012, https://celestrak.com/GPS/almanac/Yuma/.

[26] J.-C. Juang and C.-L. Chang, "Performance analysis of GPS pseudolite interference mitigation using adaptive spatial beamforming," in *Proceedings of the 61st Annual Meeting of The Institute of Navigation*, pp. 1179–1187, Cambridge, Mass, USA, June 2005.